Journal of Building Engineering 78 (2023) 107577

Contents lists available at ScienceDirect

Journal of Building Engineering

journal homepage: www.elsevier.com/locate/jobe

Application of the tying force method in the design of alternative load paths in post-and-beam timber structures: A case building

Daniele Arcuri, Simone Magatelli, Paolo Martinelli *

Department of Civil and Environmental Engineering, Politecnico di Milano, P.za L. da Vinci 32, 20133, Milan, Italy

ARTICLE INFO

Keywords:
Progressive collapse
Structural robustness
Tying force method
Alternative load path
Post-and-beam timber buildings

ABSTRACT

This work aims to present an application of the tying force method recently proposed in the literature to a mid-rise post-and-beam timber building. Internal and edge column loss scenarios are analysed. A steel-to-timber connection is proposed and extensively evaluated as a potential solution to ensure the robustness of the structure, thereby satisfying the requirements imposed by the tying force method and effectively minimizing the risk of progressive collapse of the structure. Finally, a parametric analysis evaluating the variation of the tying force as a function of the chord rotation and different beam span lengths is carried out. The results obtained show that the tying force method represents a promising and rapid strategy for designing robust post-and-beam timber buildings falling in low and medium consequence classes.

1. Introduction

Several definitions of structural robustness can be found in the literature (see but not limited to those given in Refs. [1–3]), and most of them are associated with the ability of the system to avoid structural consequences that are disproportionate with respect to the extent of the triggering initial damage. The concept of structural robustness began to interest the scientific community following the disastrous progressive collapse of the Ronan Point Tower in London in 1968 when, a gas explosion in the kitchen of a flat on the 18th floor, caused the collapse of the entire south-east corner of the building, killing four people and injuring seventeen [4]. The issue became of international interest after the events of September 11th, 2001, and the catastrophic progressive collapse of the World Trade Centre. An analysis of different failures from the point of view of robustness is reported in Agarwal et al. [5]. Over the years, structural robustness has been widely studied and analysed for concrete and steel structures, while only marginally for wood structures. Nevertheless, the potential lower environmental impact of wood compared to reinforced concrete (RC) and steel has led to the widespread use of this material in the construction field, including high-rise structures (i.e. structures characterised by having more than 8 storeys according to Ref. [6]). For a description of some of the tallest wooden buildings completed in the last decade, readers can refer to Ref. [7]. There is still, however, some scepticism about the use of wood in tall buildings over more traditional materials that are considered safer [8]. Due to the complexity of wood as a building material, the possible occurrence of risky scenarios caused by certain material criticalities is a factor that must be considered during the design process, especially in the case of high-rise buildings. Concerning the structural robustness of timber buildings, it is worth mentioning the pioneering work of Milner et al. [9] named Timber Frame project (TF2000) carried out in the UK in the late 1990s. In this work, an experimental campaign was planned to study alternative load paths after the removal of timber panels forming the walls in a six-storey light-frame timber building. More recently, Mpidi Bita et al. [10] numerically investigated the robustness of modern tall timber buildings where both a twelve-storey Cross

* Corresponding author.
E-mail address: paolo.martinelli@polimi.it (P. Martinelli).

https://doi.org/10.1016/j.jobe.2023.107577
Received 15 March 2023; Received in revised form 25 July 2023; Accepted 13 August 2023
Available online 19 August 2023

Laminated Timber (CLT) building with platform construction and a nine-storey flat-plate CLT building were analysed. The results obtained revealed that the development of catenary action within the horizontal elements is a fundamental requirement to guarantee the collapse resistance of the structure. A linear static approach was applied by Mpidi Bita et al. [11] for the analysis of a six-storey wooden office structure to guide structural designers in preventing disproportional collapse with simplified analysis tools. The behaviour of a six-storey post-and-beam mass timber building, following the removal of a vertical load-bearing element, is analysed through the application of linear static alternative load path analysis by Mpidi Bita and Tannert [12]. The work investigated three different possible failure scenarios, removal of ground floor internal, edge and corner columns, to assess whether the structural system was capable of triggering floor collapse-resistance mechanism and thus, determine possible alternative load paths for the prevention of progressive collapse. A study that represented another step towards understanding the redistribution of loads in modern timber high-rise buildings was conducted by Huber et al. [13], where a detailed finite element (FE) analysis of an eight-storey CLT building subjected to a ground floor wall removal was performed. Numerical studies were carried out also by Cao et al. [14], with the preliminary aim of estimating the dynamic amplification factors for column removal scenarios in two-dimensional (2D) timber frames. A robustness quantification of a 15-storey post-and-beam timber building through non-linear dynamic FE modelling is described in Refs. [15,16]. Three different cases of column removal on the ground floor were simulated in order to compare, through the analysis of the different robustness indices, the different performances of the building as a function of the removed element. The work of Huber et al. [17] summarises the state of knowledge about the robustness of timber structures whilst the works of Voulpiotis et al. [18] and Mpidi Bita et al. [7] present a state-of-the-art regarding structural robustness in tall timber buildings.

The theoretical and numerical studies above-mentioned have been supported in the years by few experimental investigations. Laboratory tests were conducted by Lyu et al. [19] on the collapse of a ¼-scale model reproducing glulam frames with CLT floors. A 2D frame with double span beams simulating a column loss was studied. The objective was to investigate the potential for developing catenary action using different beam-column connections. The 2D frame was tested both statically, with large deformations [19], and dynamically [20]. A subsequent experimental campaign carried out by the same research group analysed the frames in three dimensions considering the contribution of the CLT floors. Three-dimensional (3D) structures made of glulam beams and columns connected by CLT floors and subjected to a perimeter [21] and to a corner column [22] removal scenario were also tested. In these tests, two different types of connections were considered.

The draft of the upcoming Eurocode 5 *Design of Timber Structures* includes few general clauses (provisionally in *Section 4 Basis of design*) and an informative annex (provisionally named *Annex R*) addressing structural robustness and focusing on performance-based design strategies. A comprehensive description of these draft clauses is given in Ref. [23]. The importance of addressing robustness-related aspects early in the design process is emphasized in the draft Eurocode 5. This approach allows for a careful balance between robustness requirements and other design considerations. The draft Eurocode 5 also underscores that achieving robustness necessitates the implementation of suitable structural concepts and structural detailing, appropriate structural materials, and effective quality management. The performance-based design strategies included in Annex R aim to limit the total damage that may occur following assumed scenarios of initial local failure. Specifically, two key strategies are highlighted: (i) creation of alternative load paths and/or (ii) segmentation of the structure. Annex R provides guidelines for (i) designing load-carrying elements that can be removed to establish alternative load paths within the structure, and (ii) designing fuse elements that facilitate the segmentation of the structure.

The small number of studies carried out on the robustness of timber structures compared with those performed on reinforced concrete and steel stresses how this topic is relatively undeveloped, where the limited design guidance for the design of robust timber buildings represents a significant limitation for timber structural designers. In this regard, this work analyses a 6-storey post-and-beam timber structure, representing an existing building, in terms of structural robustness by making use of the recent simplified tying force method proposed by Izzuddin and Sio [24]. The building used as case study was built about 10 years ago in Italy without any structural robustness requirements. Geometry, materials and loads are assumed from the original design, while the existing beam-to-column connection is redesigned to meet robustness requirements. For confidentiality reasons, details about the building location and designers are omitted. The new tying force method analyses the minimum resistance and ductility of the structure to avoid the disproportionate collapse of the system following the loss of a vertical load-bearing element via horizontal tying.

In the following paper, section 2 reviews the simplified tying force method proposed by Izzuddin and Sio [24]. Section 3 provides a description of the case study building highlighting the main features of the materials used, the structural elements, and the connections adopted. Sections 4 and 5 report the application of the simplified tying force method in the case of the sudden loss of an internal and edge column, respectively. Parametric analyses are performed in section 6 to evaluate the variation of tying force as a function of the chord rotation and span length parameters. Finally, section 7 draws the main conclusions.

2. Review of the tying force method

2.1. Overview

Izzuddin and Sio [24] present a method for calculating the horizontal tying force for multi-storey building structures aimed at preventing/mitigating progressive collapse. The method is cast within a simplified framework similar to existing requirements in Ref. [2] but it addresses the shortcomings of such requirements via high-level features including the assessment of tying adequacy at variable ductility levels, dynamic behaviour, and the combination of different sources of tying and load combinations based on a practical superposition procedure. The method shares similar principles with the performance-based alternative load path approach as adopted in modern design codes such as the UFC code [25]. The simplified tying force method was validated with reference to RC framed structures and to a post-and-beam timber frames under a quasi-static column-removal scenario in Ref. [26] and in Ref. [27] respectively.

The general formulation of the tying force is provided by the following expression:

$$T \geq \eta \cdot \rho \cdot \left(\frac{i_f}{\overline{\alpha}}\right) \cdot P, \quad \overline{\alpha} = \frac{\alpha}{0.2}, \quad (\alpha \text{ in rad}) \tag{1}$$

where:

- $P = \sum P_j$ is the total equivalent load obtained as a superposition from all the loads applied to the system;
- $T = \sum T_k$ is the total equivalent tying force obtained as a superposition from all active tying forces within the beam/floor system;
- i_f is a tying force intensity factor that depends on the system under consideration. The intensity factor values are derived from the principle of virtual work at a fixed chord rotation of 0.2 rad and thus vary according to the configuration considered;
- $\overline{\alpha} = \alpha/0.2$ is introduced to allow for different levels of chord rotation capacity α (rad), representing the system ductility limit. The rotation capacity α is that limit beyond which tensile catenary/membrane forces can no longer be sustained, typically due to fracture of a joint, a reinforcement bar or a tying force component, and as such would represent the point at which the load resistance provided via tying forces drops significantly [24];
- η is a dynamic amplification factor allowing of sudden column/load-bearing member loss. It can assume values between 1 for linear static response to value close to 2 for linear system responses under dynamic loads and characterised by negligible damping;
- ρ is a reduction factor that allows for additional sources of resistance beyond tying action based on constant tying forces. It has a maximum value of 1 if the resistance mechanisms are purely based on tying action. If other mechanisms such as the presence of CLT panels or interaction between tying and flexural actions contribute to the redistribution of the load-bearing, ρ can have a value lower than one [28].

Eq. (1) provides the basis for checking the adequacy of the equivalent tying force T to resist the equivalent load P for the maximum normalised rotational capacity $\overline{\alpha}$ of the system. The method also provides clear indications of the minimum chord rotation value for the activation of the tying force and the ability of the surrounding structure to withstand the redistributed loads.

2.2. Tying via double-span beams

The case in which the tying is made by means of double-span beams with a negligible contribution of the floor is presented here. It is assumed that the double-span beam deforms according to a three-hinge mechanism. Fig. 1 shows the static scheme considering the case of unequal spans.

The relationship between the tying force and the applied load is obtained from a discrete equilibrium, established in terms of the equivalence between virtual internal and external work in the deformed configuration. Intensity factors i_f, equivalent tying forces T and equivalent loads P are provided in Table 1 for typical tying via beams for equal and unequal double-span configurations, while a comprehensive derivation is provided in Ref. [24]. The proposed approach allows the combination of different load distributions through the superposition principle, where the equivalent load P is obtained by simply adding up the contributions of the different load types.

2.3. Tying via floor system

The method proposed by Izzuddin and Sio [24] also provides intensity factors i_f, equivalent tying forces T and equivalent loads P for the case where the tying is provided through the floor system. Bi-directional scenarios called two-way tying, and unidirectional scenarios, called one-way tying, are considered in the case of the loss of an internal and peripheral vertical load-bearing element respectively. Because the tying via floor system is not used as alternative load path in the case study, further details of the tying via floor system are omitted here.

2.4. Interaction with the surrounding structure

The surrounding structure must be characterised by appropriate planar stiffness for the development of horizontal tying forces. Regarding the tying via beams, Fig. 2 reports the interaction of a beam affected by the loss of a supporting column with its surrounding structure, in which v_m represents the vertical displacement at the internal hinge location, while u is the total pull-in of the surrounding structure under the full tying force F. It is possible to define an upper limit on the pull-in u for a specific rotational capacity α, establishing a minimum level of planar stiffness from the surrounding structure that would enable full tying action before reaching the

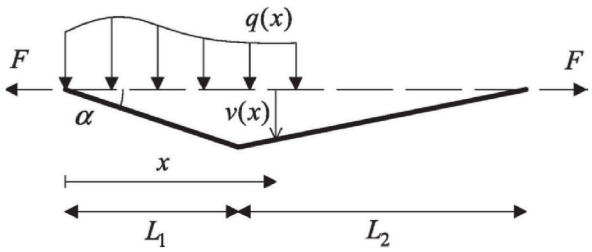

Fig. 1. Schematic representation of the tying via double-span beams (reprinted with permission from Elsevier [24]).

Table 1
Tying parameters for double-span beams (adapted from Ref. [24]).

	Equal spans	Unequal spans ($L_1 \leq L_2$)
		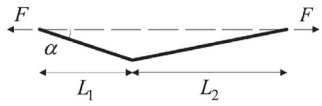
Intensity factor: i_f	2.5	$5\left(\frac{L_2}{L_1+L_2}\right)$
Equivalent tying force: T	F	F
Equivalent load: P	qL	$q\left(\frac{L_1+L_2}{2}\right)$

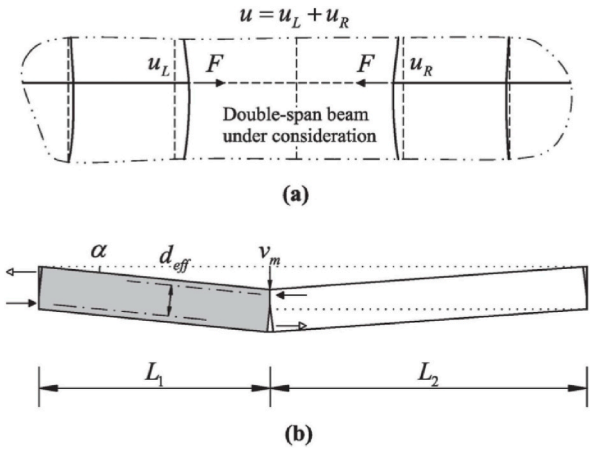

Fig. 2. Interaction of tying beam with the surrounding structure: (a) pull-in of the surrounding structure under tying force (top view); (b) deformation mode and parameters for tying via beam (reprinted with permission from Elsevier [24]).

ductility limit, by using the following expression ([24]):

$$u+\delta \leq \frac{L_1}{2}\cdot\left(\alpha-\frac{d_{\text{eff}}}{L_1}\right)^2\cdot\left(1+\frac{L_1}{L_2}\right) \tag{2}$$

In eq. (2) d_{eff} represents the distance over the cross-section between the centres of plastic rotation at the support and at the interior hinges under bending action (Fig. 2), and δ is the elastic beam elongation obtained under the full tying force.

2.5. Amplification of redistributed gravity loading

Following the removal of a load-bearing element, the amplification of gravitational loads must be considered when evaluating the surrounding structure. In this sense, Izzuddin and Sio [24] provide tabulated amplification coefficients for typical loads considered for tying via beams and the floor system.

3. Case study

3.1. Building description

A six-storey timber building for residential use is taken as a case study to apply the tying force method for the design of alternative load paths in post-and-beam timber structures. The building under study is characterised by a regular cross-shaped floor plan with a maximum length along the x-direction of approximately 44 m and a maximum length along the y-direction of approximately 34 m (Fig. 3). The building consists of six floors above ground plus a roof, reaching a total height of about 21 m (Fig. 4). The building is also characterised by the presence of a central RC core and two additional RC walls that mostly contribute to the lateral stiffening of the building. Considering the high stiffness offered by the RC core and walls, the timber structure was designed to absorb vertical loads only. Consequently, RC members were designed to carry horizontal loads resulting from seismic forces or wind actions. A simply supported scheme was generally adopted for designing timber beams. Glued laminated timber (glulam) is used in all the timber structural elements (i.e. beams, columns, and floors).

The timber columns at the ground floor are connected to a RC basement by means of metal plates and steel dowels. Along the height of the building, the columns are not continuous but are interrupted at each level. To accommodate the slab panels, the upper part of the cross-section of the main glulam beams reduces in width, as shown in Fig. 5a and Fig. 6. The beams are supported directly by the

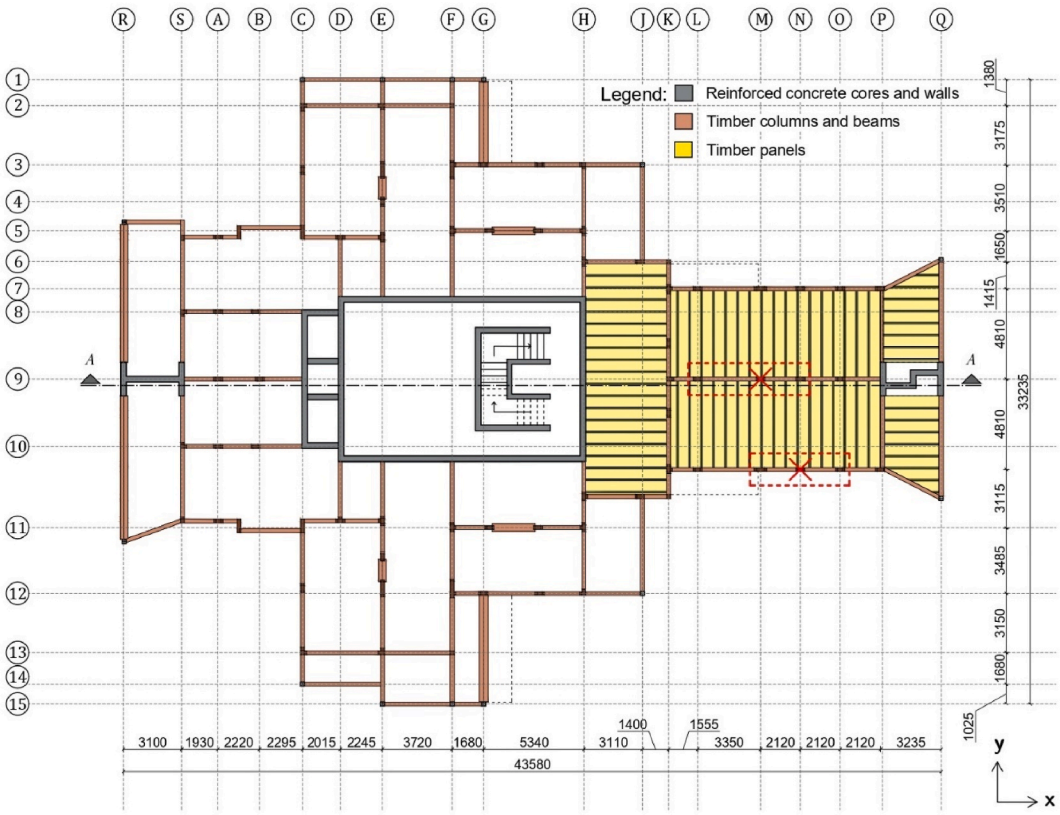

Fig. 3. Schematic plan view of the post-and-beam timber structure (unit: mm).

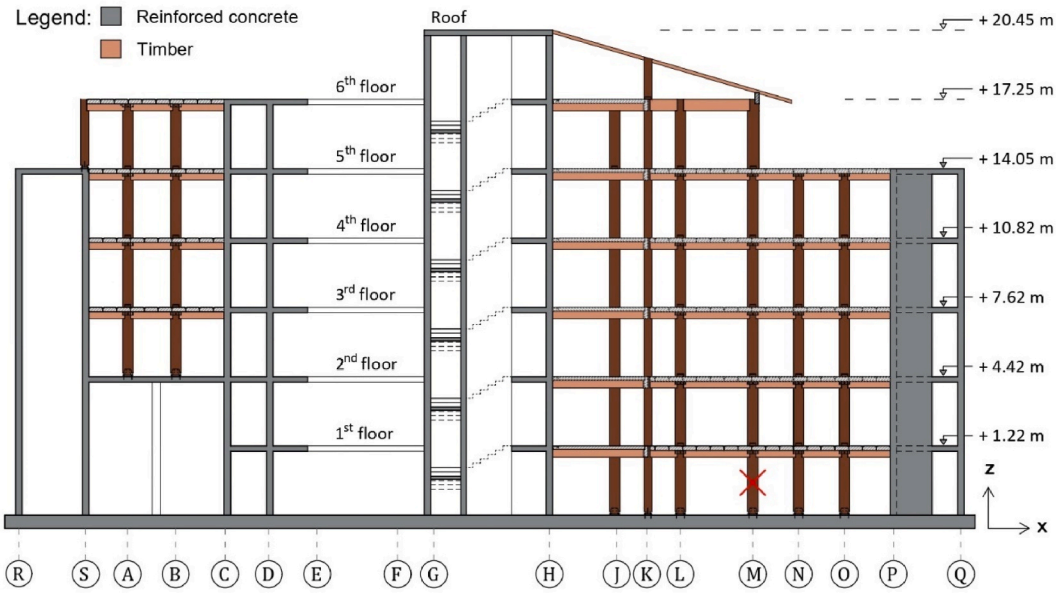

Fig. 4. Vertical section (A–A) of the post-and-beam timber structure.

vertical timber elements by means of a cross-section reduction at the top of the columns. When this solution is not applicable, the connection is made via metal links. Two strength classes of glulam, namely GL28c and GL32h [29], are used for timber columns and beams. The selection of the strength class depends on the spans of the structural elements and the applied loads. In the subsequent

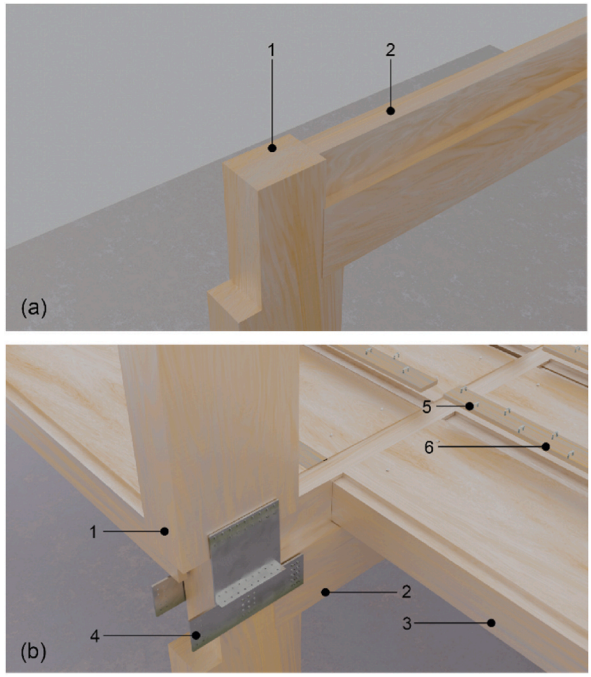

Fig. 5. Details of (a) beam-to-column and (b) beam-to-panel connections.

sections, the analysed columns and beams are all assumed to be of strength class GL28c class of wood. The floors are made of glued laminated timber panels lying side by side, class GL24h with a width of 640 mm and positioned against the main beams. Each slab panel has a cross-section reduction on both sides to allow interconnection between two adjacent panels (see Fig. 5b and Fig. 6). Slab panels are positioned on the beam notches and subsequently connected to the beams by means of two screws inserted at an angle of 45°. Following the fastening of the panels to the beams, a strip of multilayer wood is placed between the panels and connected to them by a dense stapling (Fig. 5b). This construction solution ensures adequate stability and structural continuity of the slab, as well as an even distribution of stresses along its entire surface. Moreover, it ensures adequate transmission of forces between panels and beams, preventing undesired sliding or rotation. In correspondence with the RC walls, slab panels (see for example line H in Fig. 3) and beams (see for example joint P9 in Fig. 3) are supported by angled metal plates, these last bolted to the RC walls. Subsequently, for slab panels in correspondence with the RC walls, an additional metal plate welded to the top of the plate previously fixed to the concrete wall is placed on top of the timber slab panel and then nailed to ensure a proper connection between the components. The cross-sections of the beams, columns and slab panels are presented in Fig. 6. The typical metal plate adopted at the beam-to-column node is also shown in Fig. 6.

3.2. Material properties

The strength characteristic values adopted for the glulam elements are deduced from Ref. [29] and are listed in Table 2, where $f_{m,k}$ is the characteristic bending strength, $f_{t,0,k}$ is the characteristic tensile strength parallel to the grain, $f_{v,k}$ is the characteristic shear strength, $f_{c,0,k}$ is the characteristic compressive strength parallel to the grain, $E_{0,m}$ is the modulus of elasticity parallel to the grain and ρ_k is the characteristic density.

3.3. Load analysis

The actions applied on the structural elements are calculated according to the Italian technical code [30]. For the sake of brevity, the load analysis is carried out only for the portion of the building considered in the alternative load path analysis. The following permanent and live loads are used in this work:

- structural permanent load $G_1 = 1.19$ kN/m^2, corresponding to the self-weight of the slab panels, equal to 1.19 kN/m^2;
- non-structural permanent load $G_2 = 4.30$ kN/m^2, corresponding to the superimposed dead loads, equal to 4.30 kN/m^2;
- live load $Q_k = 2.00$ kN/m^2.

The building, located in northern Italy, was designed for seismic actions characterised by a peak ground acceleration of 0.072 g.

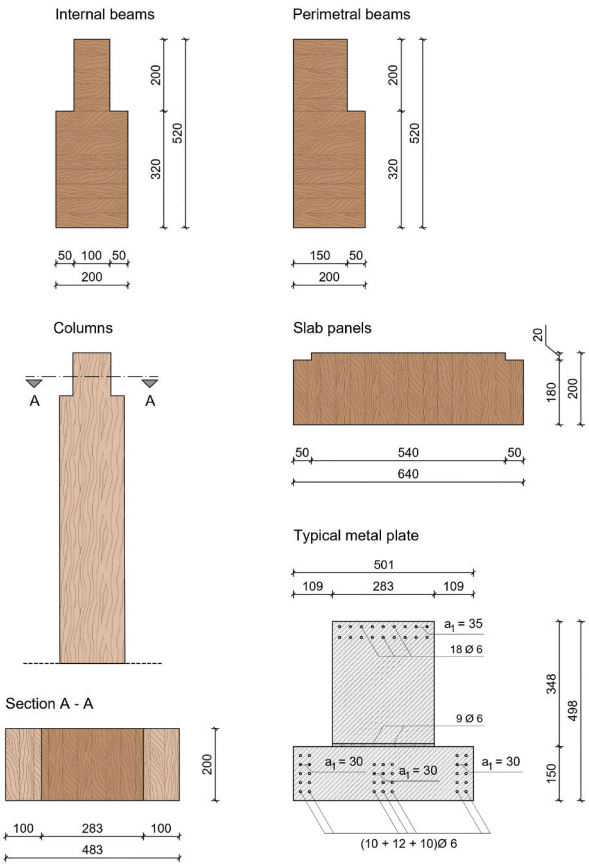

Fig. 6. Cross-sections of beams, columns and slab panels and typical metal plate detail for beam-to-column connection (unit: mm).

Table 2
Values of characteristic strengths, modulus of elasticity and density for glulam timber elements.

Material type	$f_{m,k}$ (MPa)	$f_{t,0,k}$ (MPa)	$f_{v,k}$ (MPa)	$f_{c,0,k}$ (MPa)	$E_{0,m}$ (GPa)	ρ_k (kg/m^3)
GL24h	24	16.5	2.7	24	11.6	380
GL28c	28	16.5	2.7	24	12.6	380
GL32h	32	22.5	3.8	29	13.7	430

3.4. Existing connection

Beams and columns are jointed by employing a steel-to-timber connection made of two 8 mm thick external plates properly fixed to the timber structural elements using nails with diameter (d) of 6 mm and length of 80 mm. The plate, fixed to the column with 12 nails, ensures the fastening of the beams with 10 nails and the fastening of the column above with 18 nails (Fig. 5b and Fig. 6).

4. Internal column loss scenario

4.1. Overview

Design from actions from unspecified hazards can be treated with a notional damage scenario approach, which may include (i) notional deterioration scenarios or (ii) notional element-removal scenarios. In the former case, the geometrical and/or material properties of one or more structural elements are reduced whilst in the latter case structural elements are removed. In both situations, the structural safety of the modified structure is then checked, to ensure that it can provide an alternative load path (ALP) for the applied loads. Among the structural elements that can be notionally removed, the most common are columns (one or more) and panels/walls (one or more). The notional removal scenario strategy is applied to the building under study. This strategy has been largely applied in the literature to evaluate the robustness of buildings (see for example Rodriguez et al. [31] and Martinelli et al. [32], among the others). The notional removal scenarios approach herein adopted is more conservative than the notional deterioration scenarios approach. According to CNR DT 214/2018 (§6.5.5) [33], the typical failure modes for which the design strategy for robustness is applicable are:

1. Collapse of the column only (the beam-column node remains intact): in this case, robustness exploits the coupled behaviour between:
   a) residual tensile strength of the beam-column connection which allows the activation of a catenary behaviour of the beam itself (second-order effects);
   b) membrane resistance of the slab (adequate strength must be ensure to the connections in the presence of this stress state);
2. Failure of the beam-column node: in this case, the robustness is ensured exclusively by the membrane behaviour of the slab.

In the analysis presented in the following, the collapse of the column only is assumed, leaving the node intact, thus implying that the robustness relies on the catenary action of the beam (point 1a mentioned above). Some of the causes that can lead to the sudden loss of a vertical load-bearing element or the reduction of the load-bearing capacity in timber structures are described in detail in Ref. [34]. With reference to residential wooden buildings, the loss of a column can be attributed to various factors listed below not in order of importance.

1) Blast damage: explosions in residential environments are typically due to gas leakage. A few cases of explosions associated with scooter and e-bikes batteries are also documented. The pressure wave generated by an explosion can seriously damage the column and impair its bearing capacity.
2) Fire damage: in the event of a fire, the heat can cause wooden columns to char and lose their load-bearing capacity, leading to structural failure.
3) Moisture and decay: wood is susceptible to moisture infiltration and decay. Prolonged exposure to moisture, high humidity levels, or water leaks can weaken the column's integrity, causing it to deteriorate and eventually fail.
4) Insect infestation: wood-destroying insects, such as termites or carpenter ants, can significantly compromise the structural integrity of wooden columns. These pests can hollow out or weaken the wood, making it susceptible to failure.
5) Poor workmanship or material quality: inadequate construction practices or substandard materials, can result in a weak or unstable column, making it prone to failure.
6) Structural overloading: excessive vertical or horizontal loads on the column can lead to its failure. This can occur due to poor construction practices, inadequate design considerations, or changes in the building's use or occupancy that exceed the column's capacity.
7) Foundation issues: problems with the building's foundation, such as settlement, uneven soil bearing, or inadequate support, can place excessive stress on the column, leading to its failure over time.

It is clear that each of these causes could also partially damage the connection. Thus, the assumption of column removed and node intact is a common and convenient simplification at the design stage.

In this section, the sudden loss of the internal column M9 is assumed to assess robustness of the parts of the building highlighted by the corresponding dashed red rectangle in Fig. 3. This column corresponds to the vertical load-bearing element subject to the highest load. The red cross in Fig. 3 and Fig. 4 indicates the sudden loss of the column, while the dashed red rectangle highlights the region under consideration.

4.2. Loads

The beams 9.LM and 9.MN (see Fig. 3) are characterised by a length (l_{beam}) of 3.35 m and 2.12 m respectively. The self-weight of the beams, the self-weight of the slab panels, the superimposed dead load and the live load, are equal to 0.31 kN/m, 1.19 kN/m^2, 4.30 kN/m^2 and 2.00 kN/m^2, respectively. Considering a net floor span in the y-direction equal to 4.81 m, the loads per unit length acting on the beams are equal to:

- $G_1 = 0.31 + 1.19 \cdot 4.81 = 6.04$ kN/m;
- $G_2 = 4.30 \cdot 4.81 = 20.68$ kN/m;

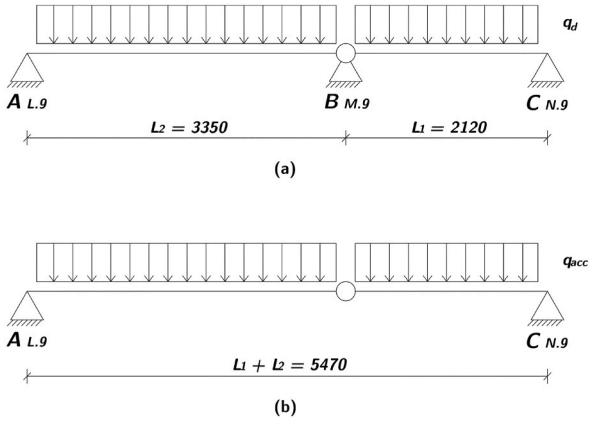

Fig. 7. Static scheme for (a) normal operating condition and (b) accidental condition in case of an internal column loss (unit: mm).

- $Q_k = 2.00 \cdot 4.81 = 9.62\ \text{kN/m}$.

Fig. 7a illustrates the static scheme of the beams 9.LM and 9.MN in normal operating conditions. In this situation, the calculation of the design load q_d, according to the Italian Code [30] (§2.6.1, Tab.2.6.I), can be expressed as:

$$q_d = \gamma_{G1} \cdot G_1 + \gamma_{G2} \cdot G_2 + \gamma_{Qi} \cdot Q_k = 1.3 \cdot 6.04 + 1.3 \cdot 20.68 + 1.5 \cdot 9.62 = 49.17\ \text{kN/m} \quad (3)$$

In the selection of the partial safety coefficient for applied loads γ_{G1}, the Italian Code (Tab.2.6.I) [30] allows to adopt the same coefficient as for the permanent structural loads ($\gamma_{G2} = \gamma_{G1} = 1.3$) if the non-structural permanent loads are fully defined.

Fig. 7b shows the static scheme of the beams when the internal column M9 (Fig. 3) is removed. In framed structures, when a column is lost and the affected floors have similar structures and loading conditions, the axial force in the columns situated directly above the removed column becomes negligible due to the redistribution effect [35]. Examples of alternative resistance mechanisms, such as catenary action in the beams and Vierendeel beam behaviour in the frame system of the upper floors, are presented in Ref. [33]. However, in the current case study, this type of redistribution effect, which is commonly observed in structures with continuous beams (e.g., RC structures), does not manifest due to the hinged behaviour of the proposed connection (see section 4.4). Therefore, the removed column scenario at the ground level requires that the upper floors also be designed to be capable of developing catenary action since equilibrium condition is achieved in the deformed configuration. In cases where the floors have similar geometry and loads, like the one studied here, the axial force in the columns located above the removed one is negligible. Consequently, it is possible to employ a simplified model, as depicted in Fig. 7b, which considers only a single floor system. To calculate the loads acting on the area considered, the accidental load combination [30] is used, giving a load value per unit length, q_{acc}, equal to:

$$q_{acc} = G_k + \psi_{21} \cdot Q_{k1} = 26.72 + 0.3 \cdot 9.62 = 29.61\ \text{kN/m} \quad (4)$$

where $G_k = 26.72$ kN/m and $Q_{k1} = 9.62$ kN/m. The coefficient ψ_{21} is assumed equal to 0.3 (Tab.2.5.I in Ref. [30]). This is valid for residential spaces. For instantaneous actions, the value of k_{mod} is 1.1 and, in the accidental load combination, the value of γ_M is 1.0 (§4.4.6. in Ref. [30]).

4.3. Determination of tying force parameters

The tying force requirement is provided by eq. (1). In the case of unequal spans ($L_1 \leq L_2$), the tying force intensity factor i_f, the equivalent load P and the equivalent tying force T are deduced from Table 1:

$$i_f = 5 \cdot \frac{L_2}{(L_1 + L_2)} = 5 \cdot \frac{3.35}{(2.12 + 3.35)} = 3.06 \quad (5)$$

$$P = q_{acc} \cdot \frac{(L_1 + L_2)}{2} = 29.61 \cdot \frac{(2.12 + 3.35)}{2} = 80.98\ \text{kN} \quad (6)$$

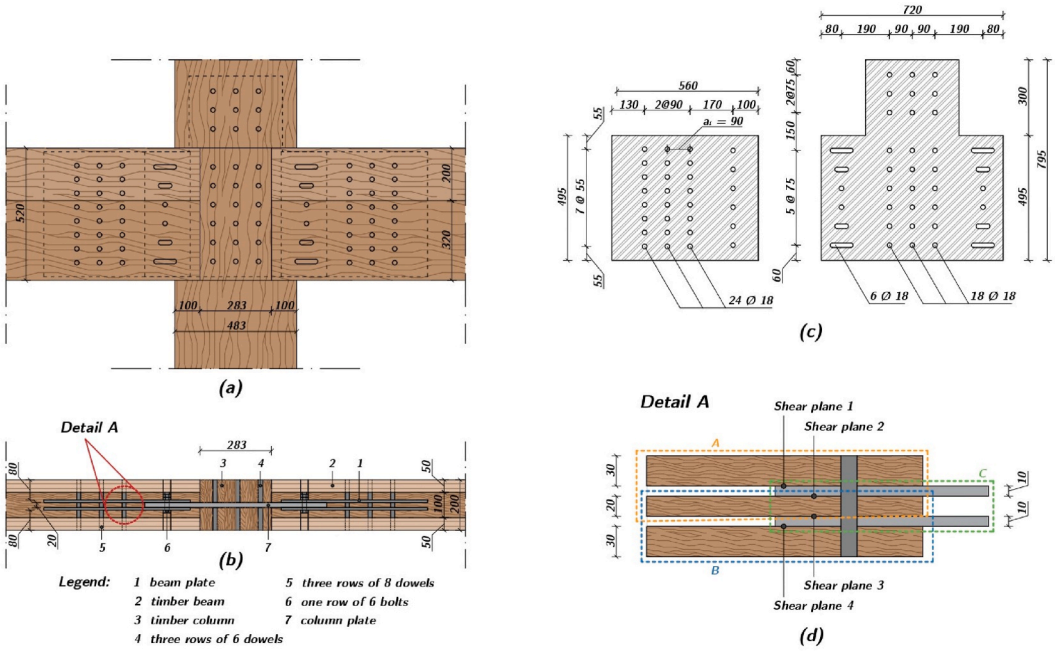

Fig. 8. Steel-to-timber connection: (a) front view, (b) horizontal section, (c) detail of steel plates and (d) detail for calculating the load-carrying capacity of the connection involving multiple shear planes (unit: mm).

$$T = F \tag{7}$$

Following a conservative approach, the contribution of additional sources of resistance as the slab panels and the compressive arch action is not considered ($\rho = 1$). Regarding the dynamic amplification factor η, a value of 1.5 is adopted. This choice is based on the numerical and experimental data so far available in the literature. According to the findings of Mpidi Bita et al. [10], dynamic simulations of a 12-story CLT building resulted in forces approximately 1.5 times higher compared to the results obtained from static analysis. Experimental tests performed on 2-bay ¼-scaled timber post-and-beam substructures resulted in average dynamic amplification factor values of 1.32 and 1.68 depending on the type of the connection [20]. Cheng et al. [20] suggest a dynamic amplification factor value of 1.5 for ductile failure modes.

The building was designed without specific considerations related to the structural robustness. The shear forces at the beam-to-column connection are entirely absorbed by the column support thank to its cross-section reduction and the existing joint metal plates (see Fig. 5b) do not meet the necessary conditions to activate the catenary mechanism. For this reason, to promote alternative load paths, a steel-to-timber connection similar to that proposed by Lyu et al. [19] is proposed and designed for the beam-to-column node to absorb the tying force under internal and edge column loss scenarios.

4.4. Assessment of connections

The steel-to-timber connection proposed by Lyu et al. [19] is selected as a potential option to enhance the robustness of the structure in comparison to the existing connection described in section 3.4. The connection was in fact specifically designed to resist the loss of a vertical load-bearing element through catenary action, enabling a ductile failure in the connection, rather than brittle failure in the timber structural elements. Considering the geometric characteristics of the beams and columns of the building under analysis (Fig. 6), some modifications, compared to the original proposal, are introduced as described below. The proposed connection depicted in Fig. 8 consists of a pair of 10 mm thick steel plates inserted into pre-cut slots in the beams (#1 in Fig. 8b) and a single 20 mm thick steel plate inserted into a pre-cut slot in the column (#7 in Fig. 8b). The three plates are connected by six M18 bolts, class 8.8 (#6 in Fig. 8b), while the connection between the two plates and the beam is realised through 24Ø18 dowels, class 8.8 with $f_{u,k} = 800$ MPa (#5 in Fig. 8b). The steel-to-timber connection proposed by Lyu et al. [19] was experimentally validated on ¼-scale tests ensuring rotation values of about 0.21 rad. Considering that the case study refers to a full-scale building and taking into account the specific changes made to the original connection, a cautionary reduced rotation value ($\alpha = 0.15$ rad) is employed in the present work. Referring to eq. (1), the required tying force corresponds to:

$$T = \eta \cdot \rho \cdot \frac{i_f}{\alpha} \cdot P = 1.5 \cdot 1 \cdot \frac{3.06}{0.75} \cdot 80.98 = 495.60 \text{ kN} \tag{8}$$

Therefore, to activate the catenary mechanism, beams and connections must provide a tensile force higher than 495.60 kN and be able to undergo rotations of at least $\alpha = 0.15$ rad without premature failure or reduction of the load-carrying capacity.

The resisting capacity of the connection is based only on steel bolts and plates and realised through six M18 bolts. It is provided by the minimum resisting mechanism among ([36]):

a) bolt shear capacity $F_{v,Rd}$;
b) plate bearing resistance $F_{b,Rd}$;
c) tension plate resistance $F_{t,Rd}$.

Mechanism (a) provides the minimum value:

$$F_{v,Rk} = 0.6 \cdot f_{ub} \cdot A_s = 0.6 \cdot 800 \cdot 192 = 92.16 \text{ kN} \tag{9}$$

where, in eq. (9) f_{ub} represents the ultimate tensile strength of the bolt and A_s is the threaded bolt area when the shear plane passes through the threaded portion of the bolt. The design bolt shear capacity ($F_{v,Rd}$) per single shear plane is obtained from:

$$F_{v,Rd} = \frac{F_{v,Rk}}{\gamma_{M2}} = \frac{92.16}{1.0} = 92.16 \text{ kN} \tag{10}$$

Based on the experimental results reported by Lyu et al. [19] and using a conservative approach, for rotation values of the joint at failure of about $\alpha = 0.15$ rad only three bolts out of six are assumed to contribute to the axial bearing capacity. Therefore, the total axial bearing capacity of the connection ($F_{v,con}$) can be determined by multiplying eq. (10) for the numbers of working bolts (3) and the number of shear planes (2):

$$F_{v,con} = F_{v,Rd} \cdot 3 \cdot 2 = 552.96 \text{ kN} \tag{11}$$

which results higher than the required tensile axial capacity calculated in eq. (8).

The connection on the beam is characterised by two slotted-in 10 mm thick steel plates and 24Ø18 dowels. For connections involving multiple shear planes, EN 1995-1-1 [37] (§8.1.3) requires that the load-carrying capacity of each shear plane be determined assuming that each shear plane is part of a series of connections among sets of three elements (see Fig. 8d). The total load-carrying capacity of the connection is then determined by calculating the sum of the minimum load-carrying capacities for each shear plane. Referring to triplet A in Fig. 8d, representing a connection characterised by a steel plate interposed as a central element of a double shear connection, the characteristic load-carrying capacity ($F_{v,Rk}$) is assumed to be the minimum among the resistance

mechanisms corresponding to modes (f), (g), and (h) (§8.2.3 of [37]):

$$F_{v,Rk} = min\begin{cases} f_{h,1,k} \cdot t_1 \cdot d & (f) \\ f_{h,1,k} \cdot t_1 \cdot d \cdot \left[\sqrt{2 + \dfrac{4 \cdot M_{y,k}}{f_{h,1,k} \cdot t_1^2 \cdot d}} - 1\right] & (g) \\ 2.3 \cdot \sqrt{M_{y,k} \cdot f_{h,1,k} \cdot d} & (h) \end{cases} \tag{12}$$

In eq. (12) t_1 represents the smaller thickness of the timber member equal to 20 mm (see Fig. 8), $f_{h,1,k}$ is the characteristic embedment strength of the timber beam calculated from §8.5.1.1 of [37] and equal to 25.55 N/mm^2, d is the fastener diameter equal to 18 mm, $M_{y,k}$ is the characteristic fastener yield moment calculated following §8.5.1.1 of [37] and equal to 440473.47 Nmm. In failure modes (g) and (h) rope effect has been neglected.

Failure mode (f) provides the minimum value:

$$F_{v,Rk,A} = 25.55 \cdot 20 \cdot 18 = 9.20 \text{ kN} \tag{13}$$

Considering that the steel-to-timber connection in triplet B is identical to that in triplet A (see Fig. 8d), it results that:

$$F_{v,Rk,B} = F_{v,Rk,A} = 9.20 \text{ kN} \tag{14}$$

Triplet C refers to a steel-to-timber connection realised with two steel plates as the outer members of a double shear connection (Fig. 8d). Considering that the plate thickness ($t_{plate} = 10$ mm) is included between $0.5d < t_{plate} < d$, with d equal to 18 mm, EN 1995-1-1 [37] (§8.2.3) recommends that the characteristic load-carrying capacity of these connections should be calculated by linear interpolation from the cases of thin and thick steel plates.

The characteristic load-carrying capacity of a steel-to-timber connection with thin steel plates as the outer members of a double shear connection is equal to the minimum between the resistant mechanisms (j) and (k):

$$F_{v,Rk} = min\begin{cases} 0.5 \cdot f_{h,2,k} \cdot t_2 \cdot d & (j) \\ 1.15 \cdot \sqrt{2 \cdot M_{y,k} \cdot f_{h,2,k} \cdot d} & (k) \end{cases} \tag{15}$$

In the case of thick steel plates as the outer members of a double shear connection, the characteristic load-carrying capacity of the connection is assumed equal to the minimum between the resistant mechanisms (l) and (m):

$$F_{v,Rk} = min\begin{cases} 0.5 \cdot f_{h,2,k} \cdot t_2 \cdot d & (l) \\ 2.3 \cdot \sqrt{M_{y,k} \cdot f_{h,2,k} \cdot d} & (m) \end{cases} \tag{16}$$

In failure modes (k) (eq. (15)) and (m) (eq. (16)), rope effect has been neglected.

Referring to eq. (15) and eq. (16), t_2 represents the thickness of the central timber element equal to 20 mm (see Fig. 8), $f_{h,2,k}$ is the characteristic embedment strength of the timber beam equal to 25.55 N/mm^2, d is the fastener diameter equal to 18 mm, $M_{y,k}$ is the characteristic fastener yield moment equal to 440473.47 Nmm.

In eq. (15) failure mode (j) provides the minimum value while in eq. (16) failure mode (l) provides the minimum value. It is worth pointing out that both failure modes, defined by the same expression, are specifically associated with the embedment failure of the connected timber component. The characteristic load-carrying capacity of triplet C corresponds therefore to:

$$F_{v,Rk,C} = 0.5 \cdot 25.55 \cdot 20 \cdot 18 = 4.60 \text{ kN} \tag{17}$$

The total characteristic load-carrying capacity of the connection ($F_{v,Rk,con}$) can thus be defined as the sum of the minimum load-carrying capacities for each shear plane:

$$F_{v,Rk,con} = F_{v,Rk,SP1} + F_{v,Rk,SP2} + F_{v,Rk,SP3} + F_{v,Rk,SP4} \tag{18}$$

where $F_{v,Rk,SP1}$ and $F_{v,Rk,SP4}$ are the characteristic load-carrying capacity related to the shear planes 1 and 4, while $F_{v,Rk,SP2}$ and $F_{v,Rk,SP3}$ are the characteristic load-carrying capacities related to the shear planes 2 and 3 (Fig. 8d). Quantities $F_{v,Rk,SP1}$, $F_{v,Rk,SP2}$, $F_{v,Rk,SP3}$ and $F_{v,Rk,SP4}$ are calculated as:

$$F_{v,Rk,SP1} = F_{v,RK,A} = 9.20 \text{ kN} \tag{19}$$

$$F_{v,Rk,SP2} = \min\left(F_{v,RK,A}; F_{v,RK,C}\right) = \min(9.20; 4.60) = 4.60 \text{ kN} \tag{20}$$

$$F_{v,Rk,SP3} = \min\left(F_{v,RK,B}; F_{v,RK,C}\right) = \min(9.20; 4.60) = 4.60 \text{ kN} \tag{21}$$

$$F_{v,Rk,SP4} = F_{v,RK,B} = 9.20 \text{ kN} \tag{22}$$

According to eq. (18), the total characteristic load-carrying capacity of the steel-to-timber connection per fastener ($F_{v,Rk,con}$) corresponds to:

$$F_{v,Rk,con} = 9.20 + 4.60 + 4.60 + 9.20 = 27.60 \text{ kN} \tag{23}$$

The design load-carrying capacity of the steel-to-timber connection ($F_{v,Rk,con}$) per fastener is equal to:

$$F_{v,Rd,con} = F_{v,Rk,con} \cdot \frac{k_{mod}}{\gamma_M} = 27.60 \cdot \frac{1.1}{1.0} = 30.36 \text{ kN} \tag{24}$$

Considering 3 connectors per row ($n = 3$) and taking into account a distance between the dowels in the grain direction equal to 90 mm (a_1, see Fig. 8c), the effective number (n_{ef}) of dowels per row is calculated from eq. (8.34) of [37]:

$$n_{ef} = \min\left(n; n^{0.9} \cdot \sqrt[4]{\frac{a_1}{13 \cdot d}}\right) = \min(3; 2.12) = 2.12 \tag{25}$$

The total axial force capacity of the connection ($F_{v,con}$) is therefore determined by multiplying eq. (24) by the effective numbers n_{ef} of bolts (2.12) and the number of rows (8):

$$F_{v,con} = 30.36 \cdot 2.12 \cdot 8 = 514.90 \text{ kN} \tag{26}$$

which is higher than the required tensile axial capacity calculated in eq. (8).

Furthermore, EN 1995-1-1 (§Annex A) [37] recommends that for steel-to-timber connections employing multiple dowel-type fasteners subjected to a force component parallel to the wood grain near the end of the timber element, supplementary checks related to potential brittle failures must be carried out. Specifically, the characteristic load-bearing capacity for fracture along the perimeter of the fastener area, known as block shear failure and plug shear failure, can be assumed as:

$$F_{bs,Rk} = \max\begin{cases} 1.5 \cdot A_{net,t} \cdot f_{t,0,k} \\ 0.7 \cdot A_{net,v} \cdot f_{v,k} \end{cases} \tag{27}$$

where $A_{net,t}$ is the net cross-sectional area perpendicular to the grain corresponding to 28,120 mm^2 and $A_{net,v}$ is the net shear area in the direction parallel to the grain equal to 80,740 mm^2. According to Table 2, $f_{t,0,k}$ and $f_{v,k}$ correspond to 16.5 N/mm^2 and 2.7 N/mm^2 respectively. Quantities $A_{net,t}$ and $A_{net,v}$ are calculated from eq. A.2 and A.3 of [37].

Referring to eq. (27), the characteristic load-carrying capacity for fracture along the perimeter of the fastener area ($F_{bs,Rk}$) corresponds to 695.97 kN, which results higher than the required tensile axial capacity calculated in eq. (8).

Fig. 9 depicts the deformed configuration of the beam-to-column node caused by the sudden column loss at the maximum chord rotation ($\alpha = 0.15$ rad). In the background, the undeformed configuration of the structure serves as a reference, enabling a comprehensive comparative analysis. The rotational displacement of the structural elements becomes apparent, accompanied by the consequential behaviour exhibited by the connection. A close-in examination of the plate further shows the displacement of the dowels within the slots, accompanied by the corresponding tensile forces acting upon them. It is evident that, with a maximum rotation of $\alpha = 0.15$ rad, four out of the six bolts are activated. Therefore, considering three active bolts when evaluating the bearing capacity of the connection ($F_{v,con}$ in eq. (11)) proves to be a conservative assumption.

While the proposed connection meets the verifications specified in EN 1995-1-1 (§Annex A) [37] regarding brittle failure modes, there are two aspects of this proposal that are generally not recommended. Firstly, the use of stocky connectors is not advisable. Secondly, the significant reduction in net cross-section area caused by the presence of holes and slots is also a concern.

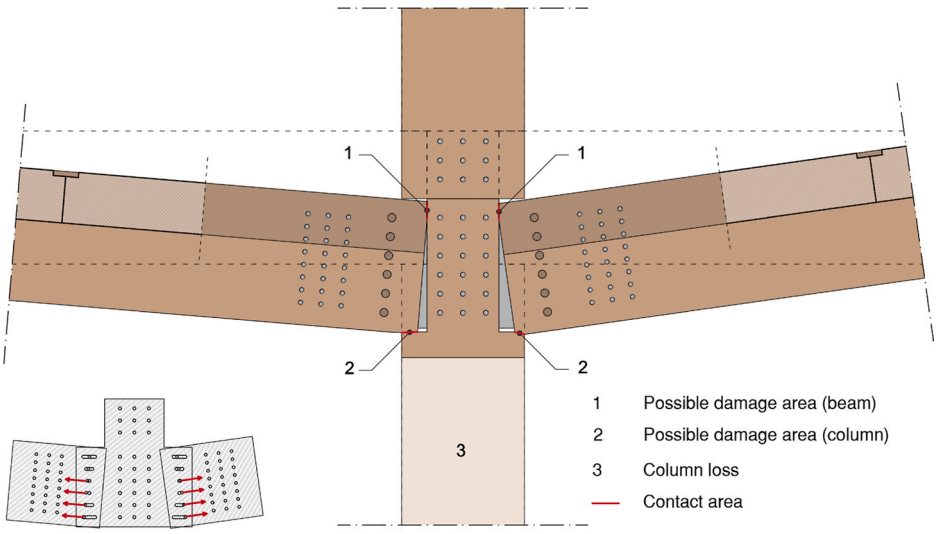

Fig. 9. Deformed configuration of the proposed steel-to-timber connection under column removal scenario.

4.5. Assessment of the timber beams

The tensile force in the beam (T_{beam}) must be sufficient to withstand the tying force T generated by the sudden loss of the column. In the timber beam assessment, the net timber cross-section ($A_{beam,net}$) is considered. The largest cross-section reduction due to the presence of the slots for the steel plates and the holes for the steel fasteners is in correspondence of the row of six M18 bolts (#6 in Fig. 8b). The tensile force in the beam can be assessed as:

$$T_{beam} = f_{t,0,d} \cdot A_{beam,net} = 18.15 \cdot 35320 = 641.06 \text{ kN} \tag{28}$$

where in eq. (28) $f_{t,0,d}$ is the design tensile strength parallel to the grain. The tensile force in the beam results higher than the required tensile axial capacity calculated in eq. (8).

Furthermore, it is important to specify that the combined bending and axial tension exerted on the beam in accidental condition meet the requirements outlined in §6.2.3 of [37].

4.6. Assessment of the surrounding structure

The surrounding structure must provide sufficient stiffness after the removal of a vertical load-bearing element. To this regard, the tying force method prescribes the application of eq. (2). Since the described connection is hinged, which implies no plastic rotation, the parameter d_{eff} in eq. (2) can be reasonably assumed to be zero.

In eq. (2) δ corresponds to the elastic extension of the beam, resulting equal to:

$$\delta = \frac{F}{EA} \cdot \frac{L_1 + L_2}{2} = \frac{495.60 \cdot 10^3}{12600 \cdot 84000} \cdot 2735 = 1.29 \text{ mm} \tag{29}$$

where the required axial force F results in this case equal to the tying force T (eq. (8)).

The application of eq. (2) leads to a maximum displacement of the surrounding structure within which full catenary action may developed equal to:

$$u \leq \frac{2120}{2} \cdot 0.15^2 \cdot \left(1 + \frac{2120}{3350}\right) - 1.29 = 37.65 \text{ mm} \tag{30}$$

It is worth to note that the combined axial displacements of both ends of the tie must be considered. In this scenario, the presence of the two reinforced concrete cores could contribute to providing sufficient stiffness to the system so that the combined axial displacements of the surrounding structure under the force F result less than 37.65 mm.

4.7. Assessment of the timber columns

The dynamic effects associated with the sudden loss of a column can be considered when evaluating the alternative load paths using the dynamic amplification factor, which establishes an equivalent amplification of the vertical loading to the surrounding structure. Izzuddin and Sio [24] provide tabulated amplification factors to be applied to the gravity loads depending on the type of scenario investigated. For the case analysed, the amplification factor results equal to $0.25 + 0.75 \times \eta = 1.375$, with η equal to 1.5.

The values of the axial force acting as a result of the redistribution of the loads on the two columns adjacent to the removed one, namely column N.9 and column L.9 (Fig. 3), are calculated in the following.

Referring to the internal column N.9, the determination of the axial force at the base of the ground floor under design conditions ($N_{d,N,9,tot}$) is obtained through the following expression:

$$N_{d,N.9,tot} = \sum_{i=1}^{n} N_{d,N.9,i} \tag{31}$$

In eq. (31), n corresponds to the number of building's storeys ($n = 5$), while $N_{d,N,9,i}$ represents the axial force in design conditions for the i^{-th} floor, calculated as follows:

$$N_{d,N.9,i} = \frac{1}{2} \cdot q_d \cdot \left(L_{b9,NO,i} + L_{b9,MN,i}\right) + W_{column,i} = \frac{1}{2} \cdot 49.17 \cdot (2.12 + 2.12) + 1.08 = 105.32 \text{ kN} \tag{32}$$

where q_d represents the design distributed load calculated in eq. (3), while the terms $L_{b9,NO,i}$ and $L_{b9,MN,i}$ refer to the lengths of beams 9.NO and 9.MN on the i^{-th} floor, respectively. Additionally, the term $W_{column,i}$ represents the self-weight of the column for the i^{-th} floor under consideration. The total axial force acting at the base of ground floor of column N.9 ($N_{d,N.9,tot}$) corresponds to 526.48 kN, resulting in an axial stress at the base of the column ($\sigma_{c,0,d,N.9}$) equal to:

$$\sigma_{c,0,d,N.9} = \frac{N_{d,N.9,tot}}{A_{column,N.9}} = \frac{526.48 \times 10^3}{96600} = 5.45 \text{ MPa} \tag{33}$$

Under the specified normal operating conditions, considering for instantaneous actions the value of k_{mod} equal to 0.8 (§4.4 in Ref. [30]) and γ_M equal to 1.45 (§4.4 in Ref. [30]), the structural verifications in terms of load-bearing capacity (§6.1.4 in Ref. [37]) and buckling (§6.3.2 in Ref. [37]) are satisfied.

In accidental load conditions, the axial force at the base of the ground floor ($N_{acc,N.9,tot}$) can be determined using the following

expression:

$$N_{\mathrm{acc,N.9,tot}} = \sum_{i=1}^{n} N_{\mathrm{acc,N.9,i}} \tag{34}$$

In eq. (34), $N_{\mathrm{acc,N.9,i}}$ represents the axial force in accidental conditions for the i$^{\text{-th}}$ floor, calculated as:

$$N_{\mathrm{acc,N.9,i}} = \frac{1}{2}\cdot q_{\mathrm{acc}}\cdot L_{\mathrm{b9,NO,i}} + 1.375\cdot\frac{1}{2}\cdot q_{\mathrm{acc}}\cdot\left(L_{\mathrm{b9,MN,i}} + L_{\mathrm{b9,LM,i}}\right) + W_{\mathrm{column,i}} = \frac{1}{2}\cdot 29.61\cdot 2.12 + 1.375\cdot\frac{1}{2}\cdot 29.61\cdot(2.12+3.35) + 1.08 = 143.82\ \mathrm{kN} \tag{35}$$

where q_{acc} represents the accidental distributed load calculated in eq. (4), while the terms $L_{\mathrm{b9,NO,i}}$, $L_{\mathrm{b9,MN,i}}$ and $L_{\mathrm{b9,LM,i}}$ refer to the lengths of beams 9.NO, 9.MN and 9.LM on the i$^{\text{-th}}$ floor respectively. In eq. (35) the double-span contribution is amplified by the factor 1.375. The total axial force acting on column N.9 in accidental load conditions ($N_{\mathrm{acc,N.9,tot}}$), is calculated as the sum of the axial forces for each floor, resulting in a value of 719.57 kN, providing an axial stress ($\sigma_{\mathrm{c,0,acc,N.9}}$) at the base of the column equal to 7.45 MPa. Therefore, under accidental load conditions, the column is subjected to an overload factor of 1.37 compared to the design conditions. However, for instantaneous actions the value of k_{mod} is 1.1 and in the accidental load conditions, γ_{M} is 1.0. As a result, the material strength values are significantly higher than those calculated based on design conditions ($k_{\mathrm{mod}} = 0.8$ and $\gamma_{\mathrm{M}} = 1.45$). Consequently, the higher material strength ensures that the column verification requirements are still satisfied even under accidental load conditions, both in terms of load-bearing capacity and buckling. Nevertheless, due to the increased axial force at the base, additional verifications of the foundation's capacity should be conducted to ensure its adequacy. Applying a similar procedure to column L.9, which is omitted here for brevity, confirms that the column also satisfies the requirements under accidental load conditions.

5. Edge column loss scenario

5.1. Loads

The simplified tying force method [24] is now applied with reference to an edge column loss scenario. The tying is provided via the double-span beams. The edge column removal simulation is carried out on the structural frame 10, as highlighted in Fig. 3. Specifically, the analysed area consists of beams 10.MN and 10.NO, while the column subjected to removal is the N.10. Beams 10.MN and 10.NO are both characterised by a length (l_{beam}) of 2.12 m. The beam self-weight, the self-weight of the slab panels, the self-weight of the external wall, the permanent load of the external wall, the superimposed dead load and the live load, are equal to 0.36 kN/m, 1.19 kN/m^2, 1.08 kN/m^2, 1.08 kN/m^2, 4.30 kN/m^2 and 2.00 kN/m^2 respectively. Considering a net floor span of 2.405 m and an inter-storey height (h_{int}) of 2.68 m, the loads per unit length acting on the beams 10.MN and 10.NO are equal to:

- $G_1 = 0.36 + 1.19\cdot 2.405 + 1.08\cdot h_{\mathrm{int}} = 6.12$ kN/m;
- $G_2 = 4.30\cdot 2.405 + 1.08\cdot h_{\mathrm{int}} = 13.24$ kN/m;
- $Q_{\mathrm{k}} = 2.00\cdot 2.405 = 4.81$ kN/m.

In the analysis presented below, the collapse of the column only is assumed, leaving the node intact. Fig. 10a shows the static scheme of the structural elements considered in normal operating conditions. In this situation, the design load q_{d} can be calculated as:

$$q_{\mathrm{d}} = \gamma_{\mathrm{G1}}\cdot G_1 + \gamma_{\mathrm{G2}}\cdot G_2 + \gamma_{\mathrm{Qi}}\cdot Q_{\mathrm{k}} = 1.3\cdot 6.12 + 1.3\cdot 13.24 + 1.5\cdot 4.81 = 32.32\ \mathrm{kN/m} \tag{36}$$

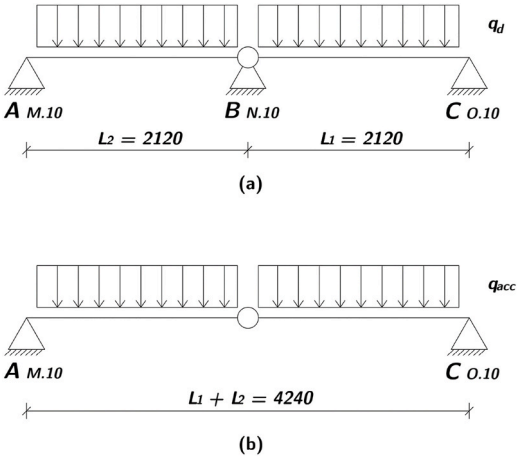

Fig. 10. Static scheme for (a) normal operating condition and (b) accidental condition in case of an edge column loss (unit: mm).

where the partial safety coefficients for the applied loads are those proposed by the Italian Code [30]. Fig. 10b shows the static scheme when the edge column is removed (column N.10 in Fig. 3). In the accidental load condition [30], the load per unit length (q_{acc}) acting on the examined beams is equal to:

$$q_{acc} = G_k + \psi_{21} \cdot Q_{k1} = 19.36 + 0.3 \cdot 4.81 = 20.74 \text{ kN/m} \tag{37}$$

where G_k and Q_{k1} are the permanent and live loads respectively, acting on the analysed area, and the coefficient $\psi_{21} = 0.3$ refers to residential buildings [30]. For instantaneous actions, the value of k_{mod} is 1.1 and, in the accidental load combination, the value of γ_M is 1.0 (§4.4.6. in Ref. [30]).

5.2. Determination of tying force parameters

The tying force requirement is provided by eq. (1). According to Table 1, for beams characterised by equal span, the tying force intensity factor (i_f) is set equal to 2.50, whilst the equivalent load P and the equivalent tying force T are calculated as:

$$P = q_{acc} \cdot L = 20.74 \cdot 2.12 = 43.97 \text{ kN} \tag{38}$$

$$T = F \tag{39}$$

Following the same approach described in section 4.3, the contribution of additional sources of resistance (i.e. slab panels and compressive arch action) is not accounted for ($\rho = 1$), and the dynamic amplification factor is set to the value of 1.5 ($\eta = 1.5$). Additionally, the same steel-to-timber connection employed for internal column loss scenario is adopted in the following, which involves the adoption of a chord rotation factor α equal to 0.15 rad (see section 4.4). Referring to eq. (1), the required tying force corresponds to:

$$T = \eta \cdot \rho \cdot \frac{i_f}{\alpha} \cdot P = 1.5 \cdot 1 \cdot \frac{2.50}{0.75} \cdot 43.97 = 219.85 \text{ kN} \tag{40}$$

Therefore, to activate the catenary mechanism, beams and connections must provide a tensile force higher than 219.85 kN and be able to undergo rotations of at least $\alpha = 0.15$ rad without premature failure or reduction of the load-carrying capacity.

5.3. Assessment of connections

The same steel-to-timber connection employed for internal column loss scenario (section 4) is adopted. For details on the calculation methodology, readers can refer to section 4.4. According to eq. (26), the total axial force capacity of the connection ($F_{v,con}$) corresponds to 514.90 kN, which is higher than the required tensile axial capacity calculated in eq. (40) equal to 219.85 kN.

5.4. Assessment of the timber beams

In the evaluation of the tensile force in the beam (T_{beam}), the same methodology as that described for the case of internal column loss scenario is followed, resulting in a value of tensile force in the beam equal to:

$$T_{beam} = f_{t,0,d} \cdot A_{beam,net} = 18.15 \cdot 45320 = 822.56 \text{ kN} \tag{41}$$

Consequently, in the event of a sudden edge column loss, the tying force capacity of the beam results higher than the required tensile axial capacity calculated in eq. (40) equal to 219.85 kN.

5.5. Assessment of the surrounding structure

The surrounding structure must provide sufficient stiffness after the removal of the vertical load-bearing element. According to section 2.4, applying eq. (2) for beams characterised by equal spans (i.e. $L_1 = L_2 = L$), the maximum displacement of the surrounding structure within which full catenary action may develop is:

$$u \leq L \cdot \left(\alpha - \frac{d_{eff}}{L}\right)^2 - \delta = 2120 \cdot 0.15^2 - 0.39 = 47.21 \text{ mm} \tag{42}$$

Given that the adopted connection is hinged, which implies no plastic rotations, d_{eff} can be reasonably assumed to be zero. The elastic extension δ of the beam is equal to:

$$\delta = \frac{F}{EA} \cdot L = \frac{219.85 \cdot 10^3}{12600 \cdot 94000} \cdot 2120 = 0.39 \text{ mm} \tag{43}$$

where F is the tensile force of the beam-to-column connection (see eq. (40)).

5.6. Assessment of the timber columns

Izzuddin and Sio [24] provide a table of amplification factors to be applied to the gravity loads depending on the type of scenario under investigation, in order to assess the dynamic effects associated with the sudden loss of a column. For the case analysed, the amplification factor turns out to be $0.25 + 0.75 \times \eta = 1.375$, with η equal to 1.5.

The values of the axial force acting as a result of the redistribution of the loads on the two columns adjacent to the removed one (i.e.

N.10), columns O.10 and M.10, are calculated in the following. Concerning the edge column O.10, the determination of the axial force at the base of the ground floor under design conditions ($N_{d,O.10,tot}$) is obtained through the following expression:

$$N_{d,O.10,tot} = \sum_{i=1}^{n} N_{d,O.10,i} \tag{44}$$

In eq. (44), n corresponds to the number of building's storeys ($n = 5$), while $N_{d,O.10,i}$ represents the axial force in design conditions for the i^{-th} floor, calculated as follows:

$$N_{d,O.10,i} = \frac{1}{2} \cdot q_d \cdot \left(L_{b10,OP,i} + L_{b10,NO,i}\right) + W_{column,i} = \frac{1}{2} \cdot 32.32 \cdot (2.12 + 2.12) + 1.08 = 69.60 \text{ kN} \tag{45}$$

where q_d represents the design distributed load calculated in eq. (36), while the terms $L_{b10,OP,i}$ and $L_{b10,NO,i}$ refer to the lengths of beams 10.OP and 10.NO on the i^{-th} floor, respectively. The total axial force acting at the base of ground floor of column O.10 ($N_{d,O.10,tot}$) is 348.65 kN, resulting in an axial stress ($\sigma_{c,0,d,O.10}$) at the base of the column equal to 3.61 MPa. Under the specified design conditions ($k_{mod} = 0.8$ and $\gamma_M = 1.45$), structural verifications in terms of load-bearing capacity and buckling are satisfied.

In accidental load conditions, the axial force at the base of the ground floor ($N_{acc,O.10,tot}$) can be determined using the following expression:

$$N_{acc,O.10,tot} = \sum_{i=1}^{n} N_{acc,O.10,i} \tag{46}$$

In eq. (46), $N_{acc,O.10,i}$ represents the axial force in accidental conditions for the i^{-th} floor, calculated as:

$$N_{acc,O.10,i} = \frac{1}{2} \cdot q_{acc} \cdot L_{b10,OP,i} + 1.375 \cdot \frac{1}{2} \cdot q_{acc} \cdot \left(L_{b10,NO,i} + L_{b10,MN,i}\right) + W_{column,i} = \frac{1}{2} \cdot 20.74 \cdot 2.12 + 1.375 \cdot \frac{1}{2} \cdot 20.74 \cdot (2.12 + 2.12) + 1.08 = 83.52 \text{ kN} \tag{47}$$

where q_{acc} represents the accidental distributed load calculated in eq. (37), while the terms $L_{b10,OP,i}$, $L_{b10,NO,i}$ and $L_{b10,MN,i}$ refer to the lengths of beams 10.OP, 10.NO and 10.MN on the i^{-th} floor, respectively. In eq. (47) the double-span contribution is amplified by the factor 1.375. The total axial force acting on column O.10 in accidental load conditions ($N_{acc,O.10,tot}$), is calculated as the sum of the axial forces for each floor, resulting in a value of 418.80 kN leading to an axial stress ($\sigma_{c,0,acc,O.10}$) at the base of the column equal to 4.34 MPa. This implies that, under accidental load conditions, the column is subjected to an overload factor of 1.20 compared to the design conditions. For the reasons already discussed in section 4.7, it results that the column is verified even under accidental conditions, while the foundations need to be carefully assessed due to the increased axial force at the base. By applying a similar procedure to column M.10, which is not included here for the sake of brevity, it can be confirmed that the column also meets the requirements under accidental load conditions.

6. Parametric analyses

The tying force method relies on the provision of a chord rotation capacity α, considered as the limit beyond which tensile catenary/membrane forces can no longer be sustained and as such would represent the point at which the load resistance provided via tying forces drops significantly [24]. The evaluation of the parameter α is, therefore, the key point for the application of the method. In the specific case of post-and-beam timber structures, the rotational capacity α strongly depends on the type of connection between beams and columns. The connection must be designed to guarantee rotation capacity, allowing the development of the catenary action capable of providing sufficient resistance to create an alternative load path. Parametric analyses are proposed in the following with the

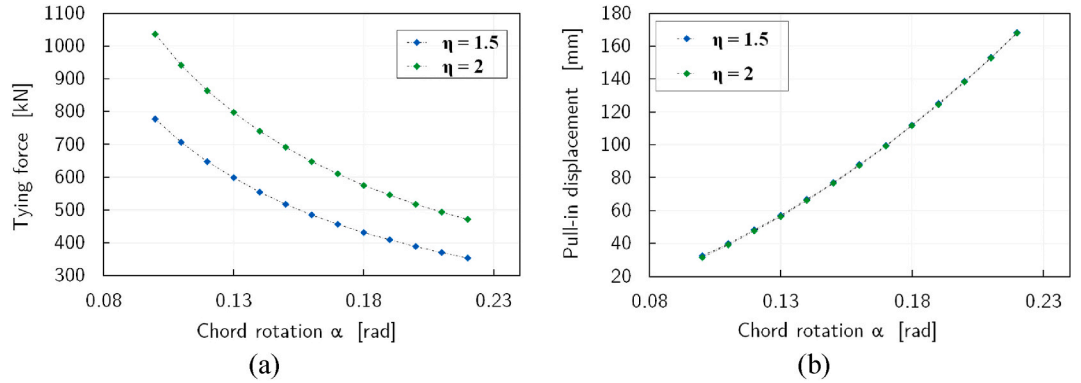

Fig. 11. (a) Required tying force as a function of the chord rotation (α); (b) total pull-in displacement of the surrounding structure (u) as a function of the chord rotation (α).

aim of analysing the effects of chord rotation and beam span length on the tying force method. The following subsections deal with the tying demand, while the details of tying capacity, which depend, for example, on the connection used, are omitted.

6.1. Variation of chord rotation (α)

A parametric analysis is first carried out for evaluating the trend of tying force required varying the parameter α. The general formulation for calculating the tying force is provided by eq. (1). For the determination of the tying forces, the parameters extracted from Table 1, which refer to the case of tying via double-span beams with equal spans ($L_1 = L_2$), are used, namely $T = F$, $i_f = 2.5$ and $P = q_{acc} \times L$. Referring to section 4, a reference accidental load (q_{acc}) equal to 29.61 kN/m is assumed. In terms of the length of the beam spans, a representative value of 3.5 m is utilized, with both L_1 and L_2 set to 3.5 m. This choice is based on the maximum observed beam span lengths in the case study (Fig. 3). Following the same approach employed in sections 4 and 5, the contribution of additional sources of resistance is not accounted for ($\rho = 1$), and the dynamic amplification factor is set to the value of 1.5 ($\eta = 1.5$; Fig. 11a – blue marks). Additionally, to highlight the impact of the dynamic amplification factor on the tying force requirement, an additional curve is included by considering a maximum value of the dynamic amplification coefficient ($\eta = 2$; Fig. 11a – green marks).

Based on the chord rotation values obtained experimentally for commercial ¼-scale steel-to-timber connections [19], a lower limit of $\alpha = 0.10$ rad is assumed. A value of $\alpha = 0.22$ rad is taken as upper limit for connections specifically designed for robust timber buildings [19]. Fig. 11a shows the required tying force as function of the chord rotations α. From the graph, it can be observed that an increase in the chord rotation capacity α leads to a considerable decrease in the tying force required with obvious consequence on the load-carrying capacity of the connection. The progressive development of the catenary action allows the structural system to maintain its load-bearing capacity even when subjected to large deformations. To fulfil the verifications imposed by the tying method, both the beam and the connection must provide a resistance higher than the tying force. The timber beam is typically able to provide an axial resistance higher than the value required by the tying force although the net cross-sectional area of the beam in proximity of the connection can be significantly reduced due to notches and holes. Conversely, the connection needs to be correctly designed to guarantee sufficient load-bearing capacity to resist the high tying force values required. Verifying the connection often turns out to be the most severe check in a column loss context. The benefits offered by connections that can develop high rotations are well observed in Fig. 11a.

Fig. 11b shows the relationship between the total pull-in displacement of the surrounding structure u and the chord rotation α. The displacement u should be understood as the limit displacement that the surrounding structure must not exceed to allow the development of the catenary action at a chord rotation α. The graph shows that an increase in the chord rotation capacity α results in an increase of the limit pull-in displacement of the surrounding structure. Furthermore, it can be observed from the graph that the two curves, for dynamic coefficient values of $\eta = 1.5$ and $\eta = 2$, are nearly overlapping. This is because in the calculation of the pull-in displacement u (eq. (2)), only the parameter δ (eq. (3)), which accounts for the elastic extension of the double-span beam, varies between the two curves, and δ is considerably smaller compared to the other terms in eq. (2).

6.2. Variation of beam span length

The effects of beam span variation on the required tying force and for different chord rotation capacities α are evaluated in this section. It is worth noting that larger beam spans result in higher total load values (as indicated in Table 1), leading to an increase in the required tying force.

The general formulation for calculating the tying force is provided by eq. (1). For the determination of the tying forces, the parameters extracted from Table 1, which refer to the case of tying via double-span beams with equal spans ($L_1 = L_2$), are used, namely $T = F$, $i_f = 2.5$ and $P = q_{acc} \times L$. Referring to section 4, a reference accidental load (q_{acc}) equal to 29.61 kN/m is assumed. Coefficients ρ and η are assumed equal to 1 and 1.5 respectively. Fig. 12 shows the required tying force when varying the beam span dimensions. It can be observed that an increase in the beam span length leads to a linear increase of the tying force required to avoid collapse. Higher values of chord rotation capacity α allow to significantly reduce the required tying force.

7. Conclusions

Providing alternative load paths is one of the ways to prevent progressive collapse of a building, under some damage scenarios. Currently, the main research effort on structural robustness is limited to reinforced concrete and steel structures, with little regard to timber structures. The aim of this work is to present an application of the tying force method developed by Izzuddin and Sio [24] to a timber building. The case study refers to an existing mid-rise post-and-beam timber building. The geometry, materials, and loads are assumed based on the original design, while the beam-to-column connection is redesigned to meet the robustness requirements. The new tying force method, while considering the required resistance via tying to the loss of a load-bearing member, preserves the simplicity of the prescriptive rules present for example in Ref. [2], but at the same time has a mechanical basis similar to that used in alternative load path analysis. The robustness of the building is analysed by simulating internal and edge column losses. Based on the results presented, the following conclusions can be drawn:

- the axial capacity of the timber beam is in general substantially higher than the axial capacity of the connections. However, in the connection region, the net cross-sectional area of the beam can be significantly reduced due to notches and holes, which can pose a check as severe as the axial tensile capacity of the connector;
- since columns are unable to transfer tensile forces perpendicular to the grain, utilizing connections that pass through the column and are fixed to the beams can be deemed as an effective solution to activate catenary action;

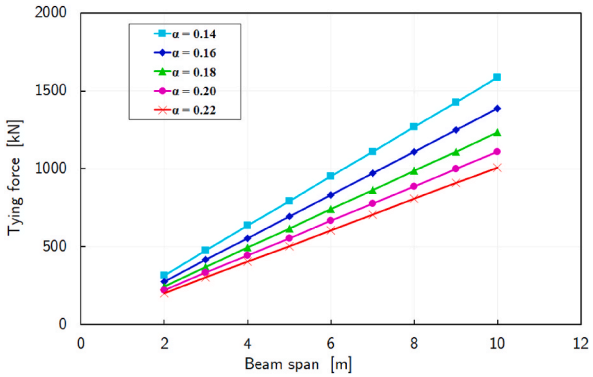

Fig. 12. Required tying force as a function of the beam span length for several values of chord rotation capacity α

- a steel-to-timber connection similar to that proposed by Lyu et al. [19] has been adopted in this study. The connection was experimentally validated on ¼-scale tests ensuring rotation values of about 0.21 rad. Cautionary reduced rotation values have been assumed in the present study, and small-scale results should be extended to full-scale connections with care;
- the contribution of CLT slab panels and the potential compressive arch action in facilitating the alternative load path and transferring loads to adjacent frames and/or connectors has been disregarded. This assumption results in conservative outcomes;
- experimental tests on timber construction systems (i.e. timber beam and column system with slab panel) are required to ensure that the connection used does not alter the hierarchy of strengths by creating undesirable damage to the columns adjacent to the removed load-bearing element;
- finally, the case study has also shown that designing earthquake-resistant structures does not automatically imply satisfying robustness requirements.

Author statement

Daniele Arcuri: Conceptualization, Methodology, Validation, Formal analysis, Writing - Original Draft, Writing - Review & Editing.

Paolo Martinelli: Conceptualization, Methodology, Validation, Formal analysis, Writing - Review & Editing, Supervision.

Simone Magatelli: Conceptualization, Methodology, Validation, Formal analysis, Writing - Original Draft, Writing - Review & Editing.

Declaration of competing interest

The authors declare that they have no known competing financial interests or personal relationships that could have appeared to influence the work reported in this paper.

Data availability

Data will be made available on request.

References

[1] GSA (General Services Administration), Alternate Path Analysis & Design Guidelines for Progressive Collapse Resistance, 2016.
[2] EN 1991-1-7, Eurocode 1 – Actions on Structures – Part 1-7: General Actions – Accidental Actions (Brussels, European Committee for Standardization), 2006.
[3] Fib. Fib Model Code for Concrete Structures 2010, Lausanne, 2013.
[4] C. Pearson, N. Delatte, Ronan point apartment tower collapse and its effect on building codes, J. Perform. Constr. Facil. 19 (2) (2005) 172–177, https://doi.org/10.1061/(ASCE)0887-3828(2005)19:2(172).
[5] J. Agarwal, M. Haberland, M. Holický, M. Sykora, S. Thelandersson, Robustness of structures: lessons from failures, Struct. Eng. Int. 22 (2012) 105–111, https://doi.org/10.2749/101686612X13216060213635.
[6] Australian Building Codes Board (ABCB), National Construction Code (NCC), Council of Australian Governments, 2016.
[7] H. Mpidi Bita, J.A.J. Huber, P. Palma, T. Tannert, Prevention of disproportionate collapse for multistory mass timber buildings: review of current practices and recent research, J. Struct. Eng. 148 (7) (2022), 04022079, https://doi.org/10.1061/(ASCE)ST.1943-541X.0003377.
[8] M. Green, J.E. Karsh, Tall Wood-The Case for Tall Wood Buildings, Report Prepared for the Canadian Wood Council on Behalf of the Wood Enterprise Coalition and Forest Innovation Investment, BC, Vancouver, 2012.
[9] M. Milner, S. Edwards, D. Turnbull, V. Enjily, Verification of the robustness of a six-storey timber-frame building, Struct. Eng. 76 (16) (1998) 307–312.
[10] H. Mpidi Bita, N. Currie, T. Tannert, Disproportionate collapse analysis of mid-rise cross-laminated timber buildings, Struct. Infrastruct. Eng. 14 (11) (2018) 1547–1560, https://doi.org/10.1080/15732479.2018.1456553.
[11] H. Mpidi Bita, R. Malczyk, T. Tannert, Alternative Load Path Analyses for Mid-rise Post and Beam Mass Timber Building, Structures Congress 2020 - Selected Papers from the Structures Congress, 2020, pp. 72–80, https://doi.org/10.1061/9780784482896.008.
[12] H. Mpidi Bita, T. Tannert, Disproportionate collapse prevention analysis for post and beam mass timber building, J. Build. Eng. 56 (2022), 104744, https://doi.org/10.1016/j.jobe.2022.104744.
[13] J.A.J. Huber, M. Ekevad, U.A. Girhammar, S. Berg, Finite element analysis of alternative load paths in a platform-framed clt building, Proc. Inst. Civ. Eng.: Structures and Buildings 173 (5) (2020) 379–390, https://doi.org/10.1680/jstbu.19.00136.

[14] A.S. Cao, P. Palma, A. Frangi, Column removal analyses of timber structures – framework to assess dynamic amplification factors for simplified design methods, in: World Conf Timber Eng, 2021, p. 2021. Online.
[15] K. Voulpiotis, Robustness of Tall Timber Buildings, Ph.D. thesis, 2021, p. 12, https://doi.org/10.3929/ethz-b-000526211.
[16] K. Voulpiotis, S. Schär, A. Frangi, Quantifying robustness in tall timber buildings: a case study, Eng. Struct. 265 (2022), 114427, https://doi.org/10.1016/j.engstruct.2022.114427.
[17] J.A.J. Huber, M. Ekevad, U.A. Girhammar, S. Berg, Structural robustness and timber buildings – a review, Wood Mater. Sci. Eng. 14 (2) (2019) 107–128, https://doi.org/10.1080/17480272.2018.1446052.
[18] K. Voulpiotis, J. Köhler, R. Jockwer, A. Frangi, A holistic framework for designing for structural robustness in tall timber buildings, Eng. Struct. 227 (2021), 111432, https://doi.org/10.1016/j.engstruct.2020.111432.
[19] C. Lyu, B. Gilbert, H. Guan, I.D. Underhill, S. Gunalan, H. Karampour, M. Masaeli, Experimental collapse response of post-and-beam mass timber frames under a quasi-static column removal scenario, Eng. Struct. 213 (2020), 110562, https://doi.org/10.1016/j.engstruct.2020.110562.
[20] X. Cheng, B. Gilbert, H. Guan, I.D. Underhill, H. Karampour, Experimental dynamic collapse response of post-and-beam mass timber frames under a sudden column removal scenario, Eng. Struct. 233 (2021), 111918, https://doi.org/10.1016/j.engstruct.2021.111918.
[21] C. Lyu, B. Gilbert, H. Guan, I.D. Underhill, S. Gunalan, H. Karampour, Experimental study on the quasi-static progressive collapse response of post-and-beam mass timber buildings under an edge column removal scenario, Eng. Struct. 228 (2021), 111425, https://doi.org/10.1016/j.engstruct.2020.111425.
[22] C. Lyu, B. Gilbert, H. Guan, I. Underhill, S. Gunalan, H. Karampour, Experimental study on the quasi-static progressive collapse response of post-and-beam mass timber buildings under corner column removal scenarios, Eng. Struct. 242 (2021), 112497, https://doi.org/10.1016/j.engstruct.2021.112497.
[23] P. Palma, R. Steiger, R. Jockwer, Addressing design for robustness in the 2nd-generation EN 1995 Eurocode 5, in: Proc., Int. Network on Timber Engineering Research (INTER), Timber Scientific Publishing, Karlsruhe, Germany, 2019.
[24] B.A. Izzuddin, J. Sio, Rational horizontal tying force method for practical robustness design of building structures, Eng. Struct. 252 (2022), 113676, https://doi.org/10.1016/j.engstruct.2021.113676.
[25] U.S. DoD, Unified Facilites Criteria (UFC) – Design of Buildings to Resist Progressive Collapse, UFC 4-023-03, 2016.
[26] S. Ravasini, J. Sio, L. Franceschini, B.A. Izzuddin, B. Belletti, Validation of simplified tying force method for robustness assessment of RC framed structures, Eng. Struct. 249 (2021), 113291, https://doi.org/10.1016/j.engstruct.2021.113291.
[27] P. Martinelli, B.A. Izzuddin, Validation and application of rational tying method for robustness design of post-and-beam timber buildings, Wood Mater. Sci. Eng. 18 (2) (2023) 363–378, https://doi.org/10.1080/17480272.2022.2035433.
[28] B.A. Izzuddin, Rational robustness design of multistory building structures, J. Struct. Eng. 148 (3) (2022), 04021279, https://doi.org/10.1061/(ASCE)ST.1943-541X.0003254.
[29] BS EN 1194, Timber Structures. Glued Laminated Timber. Strength Classes and Determination of Characteristic Values, The British Standards Institution, 1999.
[30] NTC, Norme tecniche per le costruzioni, Italy, Rome, 2018.
[31] D. Rodríguez, E. Brunesi, R. Nascimbene, Fragility and sensitivity analysis of steel frames with bolted-angle connections under progressive collapse, Eng. Struct. 228 (2021), 111508, https://doi.org/10.1016/j.engstruct.2020.111508.
[32] P. Martinelli, M. Colombo, S. Ravasini, B. Belletti, Application of an analytical method for the design for robustness of RC flat slab buildings, Eng. Struct. 258 (2022), 114117, https://doi.org/10.1016/j.engstruct.2022.114117.
[33] CNR DT 214/2018, Guide to Design of Structures for Robustness, 2021.
[34] E. Frühwald, E. Serrano, T. Toratti, A. Emilsson, S. Thelandersson, Design of Safe Timber Structures - How Can We Learn from Structural Failures in Concrete, Steel and Timber?, TVBK-3053, Division of Structural Engineering, Lund University, 2007.
[35] B.A. Izzuddin, A.G. Vlassis, A.Y. Elghazouli, D.A. Nethercot, Progressive collapse of multi-storey buildings due to sudden column loss — Part I: simplified assessment framework, Eng. Struct. 30 (5) (2008) 1308–1318. https://doi.org/10.1016/j.engstruct.2007.07.011.
[36] EN 1993-1-8, Eurocode 3, Design of Steel Structures – Part 1-8: Design of Joints, Brussels, European Committee for Standardization, 2005.
[37] EN 1995-1-1, Eurocode 5, Design of Timber Structures – Part 1-1: General - Common Rules and Rules for Buildings, Brussels, European Committee for Standardization, 2004.